fractal and fractional

Article

A Computational Method for Solving Nonlinear Fractional Integral Equations

Rajaa T. Matoog [1], Amr M. S. Mahdy [2,3,*], Mohamed A. Abdou [4] and Doaa Sh. Mohamed [2]

[1] Mathematics Department, Faculty of Sciences, Umm Al-Qura University, Makkah 24382, Saudi Arabia; rmatoog_777@yahoo.com or rtmatoog@uqu.edu.sa
[2] Department of Mathematics, Faculty of Science, Zagazig University, Zagazig 44519, Egypt; doaashokry203@yahoo.com or doaashokry@zu.edu.eg
[3] Department of Mathematics & Statistics, College of Science, Taif University, P.O. Box 11099, Taif 21944, Saudi Arabia
[4] Department of Mathematics, Faculty of Education, Alexandria University, Alexandria 21526, Egypt; abdella_777@yahoo.com or abdella_777@alexu.edu.eg
* Correspondence: amr_mahdy85@yahoo.com or amr_mahdy85@zu.edu.eg or amattaya@tu.edu.sa

Abstract: This article solves the nonlinear fractional integral equation (NFrIE) using the Genocchi polynomial method (GPM). We have provided proof to demonstrate the existence of a unique solution to the second sort of NFrIE in Hilbert space. The proof of the stability of the error has been described and discussed. These criteria are proven given the spectrum characteristics of a linear self-adjoint operator. Numerous applications, unique conditions, and specific situations are developed. Additionally, numerical examples are constructed to illustrate the efficiency and applicability of the method. Maple 18 software is utilized for the computation of all the numerical outcomes.

Keywords: nonlinear fractional integral equation; Genocchi polynomial method; existence and uniqueness; spectrum relations; stability of error; self adjoint operator

MSC: 45M10; 65R20

check for updates

Citation: Matoog, R.T.; Mahdy, A.M.S.; Abdou, M.A.; Mohamed, D.S. A Computational Method for Solving Nonlinear Fractional Integral Equations. *Fractal Fract.* **2024**, *8*, 663. https://doi.org/10.3390/fractalfract8110663

Academic Editors: Jordan Hristov, Yuri Dimitrov, Venelin Todorov and Slavi Georgiev

Received: 22 September 2024
Revised: 8 November 2024
Accepted: 11 November 2024
Published: 14 November 2024

1. Introduction

The vast array of applications in pure and applied mathematics, including in physics, fluid mechanics, electrodynamics, nonlinear biological systems, and other scientific and engineering domains, has drawn the interest of numerous researchers in fractional differential (FD) and integral equations (IEs) in recent years. Many different numerical methods have been proposed for solving FD and IEs in recent years. In [1], Hamdan et al. used Haar Wavelet for solving Volterra FIE. In [2], Pu and Fasondini presented Jacobi polynomials to obtain the solution of NFrIE. Bekkouche et al. in [3] introduced the solution to the fractional boundary value problem by using the trapezoidal rule. In [4], Mahdy et al. applied least squares and shifted Legendre methods for solving NFrIE. Alsulaiman et al. [5] used the Bernoulli matrix approach to solve NrIE. In [6], Alharbi et al. used the Haar Wavelet technique to solve FDEs. Mohamed et al., in [7], presented Chebyshev polynomials of the sixth kind for solving fractional mixed nonlinear partial integro-differential problems. Lagrange interpolation was utilized by Zabidiet al. in [8] to solve FDEs. In [9], Yi et al. developed a time-stepping algorithm for solving FDEs. Also, NFrDEs and their applications have been considered in many articles; for example, in [10], Jassim and Hussein presented the Hussein method for solving NFrDEs. In [11], Mohamed et al., the Elzaki transform method and the Homotopy perturbation method were used for solving NFrDEs. Rashid et al. [12], studied the solution of NFrDEs via fixed point theory. Lydia et al. [13] used the Kharrat–Toma iterative method to obtain the solution of NFrDEs. In [14], Yu presented Jumarie-modified Riemann–Liouville fractional calculus for solving NFrDEs.

In the present paper, GPM is applied to solve NFrIE, where GPM converts the problem to a system of algebraic equations that can be solved using numerical techniques. Finally, to demonstrate the applicability and validity of the method, we examine some numerical examples. The GPM is not based on orthogonal functions but belongs to a larger family class of polynomials: the Appell polynomial family. The advantage of GPM is its simplicity, and this method often leads to linear systems, which can be solved using numerical techniques, thus reducing computational costs and improving efficiency. However, the choice of collocation points plays an important role in obtaining accurate results. There are many applications of GPM; for example, in [15], GPM was applied for solving fractional partial integro-differential equations. In [16], GPM was used for solving fractional weakly singular IE. In [17], GPM was introduced to obtain the solution of FIDE. GPM was applied to find the solution of nonlinear Volterra integral equations with weakly singular kernels in [18]. Using the GPM matrix approach, Volterra IEs were solved in [19]. Heydari and Zhagharian [20] used GPM to obtain the solution of fractional Fornberg–Whitham equations. Loh et al. [21] presented the solution of Fredholm–Volterra fractional integro-differential equations via GPM. In [22], Seghiri et al. used GPM to obtain the solution of high-order Fredholm integro-differential equations. In [23], Mustapha used GPM for solving integro-differential equations. In [24], Isah and Phang applied GPM to obtain the solution of NFrDEs.

In this paper's remaining sections are the following. In Section 2, we present some preliminaries and basic information about Riemann –Liouville fractional integrals and Caputo fractional derivatives. In Section 3, applications and special cases of NFrDE are discussed. The existence and uniqueness of the solutions are discussed in Section 4. In Section 5, we studied the stability of error. In Section 6, the Genocchi polynomial method is applied for solving NFrDEs of the second kind. To explain the method in all instances of the error estimated using Maple 18, Section 7 offers a few numerical examples. Finally, a Discussion of the results is presented in Section 8.

In the Hilbert space $L_2(0,a]$, consider the second type of NFrDE:

$$\frac{d^{\alpha}}{dt^{\alpha}}[T\varphi(t)-\mu\varphi(t)]-M(t)\gamma(t,\varphi(t))=f(t),\quad (T\varphi(0)=\mu\varphi(0)),\quad (0<\alpha<1, t\in(0,a]). \tag{1}$$

Here, $T: H \to H$ is a linear self-adjoint operator in the Hilbert space, $\varphi : R^{+} \to H$ is an unknown function, $\gamma(t,\varphi(t))$ is a known function; μ is a constant, may be complex, and has many physical meanings, and $M, f : R^{+} \to H$ are given functions.

In this article, the convergence and the uniqueness of the solution of Equation (1) will be proved under certain relations. One can deduce several special situations and reach novel outcomes. Error estimate computation is carried out while also taking error stability into account.

The reader is referred to [25] and [26] for the existence of theorems about the FrDE. For reader reference, we direct them to [27] and [28] for descriptions of FI and its derivatives with fundamental characteristics.

2. Preliminaries and Basic Information

The following definitions and characteristics are provided for the reader's convenience.

Definition 1. *The Riemann–Liouville (RL) of order $\alpha > 0$ of a function $h : (0,\infty) \to R$ is presented by*

$$I^{\alpha}_{0^+}h(t)=\frac{1}{\Gamma(\alpha)}\int_0^t (t-s)^{\alpha-1}h(s)ds. \tag{2}$$

under the condition that the R.H.S. is point-wise established on $(0,\infty)$.

Definition 2. *The Caputo fractional derivatives of order $\alpha > 0$ of a function $g : (0,\infty) \to R$ provide*

$$D^{\alpha}_{0^+}g(t)=\frac{1}{\Gamma(n-\alpha)}\int_0^t \frac{g^{(n)}(s)}{(t-s)^{\alpha-n+1}}ds. \tag{3}$$

For the NFrDE (1) after integrating and using RL (2), we have

$$T\varphi(t) - \mu\varphi(t) - \frac{1}{\Gamma(\alpha)} \int_0^t (t-s)^{\alpha-1} M(s)\gamma(s, \varphi(s))ds = F(t), \quad t \in (0, a], \tag{4}$$

$$F(t) = \frac{1}{\Gamma(\alpha)} \int_0^t (t-s)^{\alpha-1} f(s)ds.$$

Formula (4) represents an NFrIE of the second kind.

Definition 3. *We say that* $f \in N^{\alpha}(R_+, N), \alpha > 0$ *if* $f : R_+ \longrightarrow H$ *is continuous on the half line* $t \geq 0,\ f(0) = 0$ *and*

$$\|f\|_{\alpha} = \sup_{t>0}(t^{-\alpha}\|f\|_H),$$

$$\|f\|_{L_2(0,a)} = \left\{ \int_0^a f^2(t)dt \right\}^{\frac{1}{2}}.$$

Lemma 1 (Without proof [29]). *In* $L_2([0, a])$ *space, the self-adjoint compact operator* $K\phi$ *may be expressed as follows;* $K\phi_n = \rho_n\phi_n,\ n > 0$, *where the eigenvalues and eigenfunctions are denoted by* ρ_n *and* ϕ_n, *respectively.*

3. Applications and Special Cases

Many applications and special cases can be derived from Equation (1) and its corresponding Equation (4).

First application: The following IE is taken into consideration as a significant application in the Hilbert space $L_2(0, a]$.

$$\int_0^t G(\alpha, t, s)\gamma(s, \varphi(s))ds + \int_0^a k(t, z)\varphi(z)dz - \mu\varphi(t) = f(t), \tag{5}$$

with

$$G(\alpha, t, s) = \frac{1}{\Gamma(\alpha)}(t-s)^{\alpha-1}M(s), \quad 0 < z \leq a, t \in (0, a].$$

The equation in Formula (5) is referred to as an IE of the second kind when $\mu =$ constant $\neq 0$, but it is termed the nonlinear Fredholm Volterra IE of the first kind when $\mu = 0$.

In the contact problem and creep theory, the IE (5) emerges in the nonlinear situation $\gamma(t, \varphi(t))$ or the linear status where $\gamma(t, \varphi(t)) = \varphi(t)$. Some elastic material bases are related to the kernels $G(t, s), k(t, z)$ of Fredholm integral terms and Volterra integral terms, respectively. The deformation body's elastic characteristics are described by the value μ. The function $f(t)$ describes this body. Further details about the physical interpretation of Equation (5) and its applications, involving various techniques for solutions, are available in [29].

Second application: The Boltzmann fractional equation

$$G(t)\varphi(t) + \frac{\partial^{\alpha}}{\partial t^{\alpha}}\left(\int_0^1 k(t, z)\varphi(z)dz - \mu\varphi(t)\right) = 0, \tag{6}$$

is derived at $\gamma(t, \varphi(t)) = \varphi(t), f(t) = 0$.

Many applications can be derived from Equation (6) in astrophysics, quantum mechanics, and laser theory.

If the operator T is differentiable, for example, then

$$\left[\frac{d}{dt} - \mu\right]\varphi(t) - I^{\alpha}_{0^+}M(t)\gamma(t, \varphi(t)) = f(t), \tag{7}$$

it represents an integro-differential equation of the first order and second kind.

Many special topics can be derived from the principal equation if the operator T is differentiable.

4. Existence and Uniqueness Solution

We shall demonstrate in this section that, under specific circumstances, there exists a unique solution to Equation (1).

The following presumptions are what we established for this goal:

(i) $M(s)$ has a continuous function on R^+ and fulfills

$$A(t) = \sup_{0 \le s \le t} \|M(s)\| < \infty, \quad t \in (0, a].$$

(ii) Characterize $\sigma(T)$ to represent the spectrum of the self-adjoint compact operator T and $\|.\|_t = \sup_{0 \le s \le t} \|.\|$.

(iii) Suppose that the interval $(0, a]$ contains a bounded function $f(t)$.

(iv) The established function $\gamma(t, \varphi(t))$ fulfills

(iv-a)$\|\gamma(t, \varphi(t))\|_t \le F_1 \|\varphi(t)\|_t$;.

(iv-b)$\|\gamma(t, \varphi_1(t)) - \gamma(t, \varphi_2(t))\|_t \le F_2 \|\varphi_1(t) - \varphi_2(t)\|_t$, where F_1 and F_2 are constants with $F > F_1$ and $F > F_2$.

We investigated the existence of a unique solution for NFrIE (1), so we considered

$$\Psi(t) = (T - \mu I)\varphi(t), \tag{8}$$

where I is a unit matrix.

Here, the resolvent, $R_\mu = (T - \mu I)^{-1}$, of T exists. Furthermore, the resolvent has bounds for any $\mu \in T(t)$, and the norm is defined by

$$N(t) = \sup_{\mu \in T(t)} \|R_\mu\|. \tag{9}$$

Theorem 1. *The NFrIE (1) has a convergence and unique solution according to the status*

$$FN(t)A(t)t^\alpha < \Gamma(\alpha + 1), \qquad F > F_2. \tag{10}$$

Furthermore, the norm of the solution to (1) is provided as

$$\|\varphi(t)\|_H \le \frac{\Gamma(\alpha + 1)A(t)\|f\|_t}{[\Gamma(\alpha + 1) - FN(t)A(t)t^\alpha]}.$$

Proof. First, to prove the convergence of Equation (1), assume that

$$\frac{d^\alpha}{dt^\alpha}[T - \mu I]\varphi(t) = f(t) + M(t)\gamma(t, \varphi(t)),$$

and assume that

$$[T - \mu I]\varphi(t) = \frac{1}{\Gamma(\alpha)} \int_0^t (t - s)^{\alpha - 1} M(s)\gamma(s, \varphi(s))ds + \frac{1}{\Gamma(\alpha)} \int_0^t (t - s)^{\alpha - 1} f(s)ds.$$

Let

$$(T - \mu I)\varphi(t) = \zeta(t). \tag{11}$$

Hence, we can rewrite Equation (1) in the form

$$\zeta(t) - \frac{1}{\Gamma(\alpha)} \int_0^t (t-s)^{\alpha-1} M(s) \gamma\big(s, R_\mu \zeta(s)\big) ds = F(t), \qquad F(t) = \frac{1}{\Gamma(\alpha)} \int_0^t (t-s)^{\alpha-1} f(s) ds. \tag{12}$$

Write Equation (12) in the integral operator form

$$\zeta_n(t) = \frac{1}{\Gamma(\alpha)} \int_0^t (t-s)^{\alpha-1} M(s) \gamma\big(s, R_\mu \zeta_{n-1}(s)\big) ds + F(t), \tag{13}$$

$$\zeta_{n-1}(t) = \frac{1}{\Gamma(\alpha)} \int_0^t (t-s)^{\alpha-1} M(s) \gamma\big(s, R_\mu \zeta_{n-2}(s)\big) ds + F(t). \tag{14}$$

Then,

$$\zeta_n(t) - \zeta_{n-1}(t) = \frac{1}{\Gamma(\alpha)} \int_0^t (t-s)^{\alpha-1} M(s) \big\{ \gamma\big(s, R_\mu \zeta_{n-1}(s)\big) - \gamma\big(s, R_\mu \zeta_{n-2}(s)\big) \big\} ds.$$

Let

$$\psi_n = \zeta_n(t) - \zeta_{n-1}(t) \Longrightarrow \zeta_n(t) = \sum_{i=0}^{n} \psi_i, \qquad \psi_0 = \zeta_0(t) = F(t). \tag{15}$$

Hence, we obtain

$$\|\psi_n\| = \| \frac{1}{\Gamma(\alpha)} \int_0^t (t-s)^{\alpha-1} M(s) \big\{ \gamma\big(s, R_\mu \zeta_{n-1}(s)\big) - \gamma\big(s, R_\mu \zeta_{n-2}(s)\big) \big\} ds \| \leq \frac{F_2 N(t) A(t) t^\alpha}{\alpha \Gamma(\alpha)} \|\psi_{n-1}\|,$$

where $N(t)$ is given by Equation (9).

Hence, we obtain

$$\|\psi_n\| \leq \frac{F_2 N(t) A(t) t^\alpha}{\alpha \Gamma(\alpha)} \|\psi_{n-1}\|.$$

Applying the Picard technique, followed by the conditions (i)–(v-a), Formula (15) produces

$$\|\psi_n\|_H \leq (\rho)^n \|F(t)\|, \quad \rho = \left(\frac{F_2 N(t) A(t) t^\alpha}{\Gamma(\alpha+1)} \right). \tag{16}$$

This constraint causes the series $\{\psi_n\}$ to converge under condition (9), allowing us to write

$$\|\zeta(t)\|_H = \sum_{n=0}^{\infty} \|\psi_n(t)\|_H \leq \sum_{n=0}^{\infty} \|F\| (\rho)^n = \|F\| (1-\rho)^{-1}, \rho < 1. \tag{17}$$

The above inequality (17) is convergent under the condition (10). In addition, this sequence represents the general solution as $n \to \infty$. Hence, the convergence of the solution is proved. □

Second, to prove the uniqueness of the solution, we can write Equation (12) in the integral operator form

$$\zeta(t) = K\zeta(t) = L\zeta(t) + F(t), \tag{18}$$

where

$$L\zeta(t) = \frac{1}{\Gamma(\alpha)} \int_0^t (t-s)^{\alpha-1} M(s) \gamma\big(s, R_\mu \zeta(s)\big) ds. \tag{19}$$

Then, we must prove the following two lemmas.

Lemma 2. *The integral operator $K\zeta(t)$, under the conditions (i)–(iv-a) maps the space H into itself.*

Proof. From (19), we can write

$$\|L\zeta(t)\| = \frac{1}{\Gamma(\alpha)}\| \int_0^t (t-s)^{\alpha-1} M(s)\gamma\big(s, R_\mu \zeta(s)\big)ds\|.$$

After using the Cauchy–Schwartz inequality and conditions (i)–(iv-a), we obtain

$$\|L\zeta(t)\| \leq \rho\|\zeta(t)\|, \quad \rho = \left(\frac{F_2 N(t) A(t) t^\alpha}{\Gamma(\alpha+1)}\right). \tag{20}$$

From inequality (20), we deduce that the integral operator $L\zeta(t)$ is bounded. After writing (18) in the norm form, and using inequality (20), we obtain

$$\|K\zeta(t)\| \leq \|\rho\zeta(t)\| + \|F(t)\|. \tag{21}$$

Inequality (21) shows that the operator K maps the ball S_σ into itself where the radius of the sphere $\sigma = \frac{\|F(t)\|}{1-\rho} > 0$. Hence, we have

$$\rho = \left(\frac{F_2 N(t) A(t) t^\alpha}{\Gamma(\alpha+1)}\right) < 1.$$

□

Lemma 3. *The integral operator $K\zeta(t)$ under the conditions (i)–(ivb) is continuous.*

Proof. Assuming $\zeta_1(t)$ and $\zeta_2(t)$ have two distinct solutions for Equation (12) in the Hilbert space, the continuity of the solution may be investigated. Thus, we can obtain

$$\|K(\zeta_1 - \zeta_2)(t)\| = \frac{1}{\Gamma(\alpha)}\| \int_0^t (t-s)^{\alpha-1} M(s)\{\gamma\big(s, R_\mu \zeta_1(s)\big) - \gamma\big(s, R_\mu \zeta_2(s)\big)\}ds\|.$$

After applying the Cauchy–Schwartz inequality and using conditions (i)–(iv-b), we have

$$\|K(\zeta_1 - \zeta_2)(t)\| \leq \rho\|(\zeta_1 - \zeta_2)(t)\|.$$

Hence, the integral operator K is continuous and, by extension, the integral operator L is also continuous. Moreover, since $\rho < 1$, then the integral operator K is a contraction mapping. □

5. The Stability of Error

To discuss the stability of error, assume we have a numerical solution in the form

$$\zeta_n(t) - \frac{1}{\Gamma(\alpha)} \int_0^t (t-s)^{\alpha-1} M(s)\gamma\big(s, R_\mu \zeta_n(s)\big)ds = F_n(t). \tag{22}$$

Then, we have

$$R_n(t) - \frac{1}{\Gamma(\alpha)} \int_0^t (t-s)^{\alpha-1} M(s)\big[\gamma\big(s, R_\mu \zeta(s)\big) - \gamma\big(s, R_\mu \zeta_n(s)\big)\big]ds = H_n(t), \tag{23}$$

where

$$R_n(t) = \zeta(t) - \zeta_n(t), \qquad H_n(t) = F(t) - F_n(t).$$

The above formula can be adapted, after applying the conditions (i–iii) and (iv-b) to take the form

$$\|R_n(t)\| \leq \left(\frac{F_2 N(t) A(t) t^\alpha}{\Gamma(\alpha+1)}\right)\|R_n(t)\| + \|H_n(t)\|. \tag{24}$$

The above inequality can be adapted in the form

$$\|R_n(t)\| \leq \frac{\|H_n(t)\|}{\left(1 - \frac{F_2 N(t) A(t) t^{\alpha}}{\Gamma(\alpha+1)}\right)} = \sigma. \quad (25)$$

Inequality (25) shows that the operator R maps the ball S_σ in the Hilbert space into itself. The radius of the sphere is

$$\sigma = \frac{\|H_n(t)\|}{\left(1 - \frac{F_2 N(t) A(t) t^{\alpha}}{\Gamma(\alpha+1)}\right)}.$$

Since $\sigma > 0, \|H_n(t)\| > 0$, then $\frac{F_2 N(t) A(t) t^{\alpha}}{\Gamma(\alpha+1)} < 1$.

Hence, the error $R_n(t)$ is bounded and stable according to the status $F_2 M(t) A(t) t^{\alpha} < \Gamma(\alpha+1)$.

Furthermore, for the continuity of the error, it is not difficult to prove that for the two functions of error R_{n_1}, R_{n_2}, we have

$$\|R_{n_1}(t) - R_{n_2}(t)\| \leq \left(\frac{F_2 N(t) A(t) t^{\alpha}}{\Gamma(\alpha+1)}\right) \|R_{n_1}(t) - R_{n_2}(t)\|.$$

The above inequality describes the continuity of the error. Moreover, the operator of error is a contraction according to the status $F_2 N(t) A(t) t^{\alpha} < \Gamma(\alpha+1)$, so the error has a unique representation.

6. Genocchi Polynomial Method

6.1. Properties of Genocchi Polynomials

The Genocchi numbers G_n and Genocchi polynomials (GPs) $G_n(t)$ are often described using the formulas for exponential generating $S(\xi)$ and $S(\xi, t)$, respectively, as follows:

$$S(\xi) = \frac{2\xi}{e^{\xi} + 1} = \sum_{q=0}^{\infty} G_q \frac{\xi^q}{q!}, \quad (|\ \xi\ | < \pi),$$

$$S(\xi, t) = \frac{2\xi e^{\xi t}}{e^{\xi} + 1} = \sum_{q=0}^{\infty} G_q(t) \frac{\xi^q}{q!}, \quad (|\ \xi\ | < \pi),$$

where $G_q(t)$ is GPs of order q. Also, GPs can be determined as follows:

$$G_q(t) = \sum_{k=0}^{q} \binom{q}{k} G_{q-k} t^k = 2B_q(t) - 2^{q+1} B_q(t), \quad (26)$$

and the following relationship yields the Genocchi number G_{q-k}:

$$G_q = 2(1 - 2^q) B_q,$$

where B_q is the famous Bernoulli number and $B_q(t)$ is Bernoulli polynomials.

The generating function for the Bernoulli numbers is

$$\frac{x}{e^x - 1} = \sum_{n=0}^{\infty} \frac{B_n}{n!} x^n = B_0 + xB_1 + \frac{x^2}{2!} B_2 + \ldots + \frac{x^n}{n!} B_n + \ldots.$$

Bernoulli numbers are defined as follows:

$$B_n^- = \sum_{k=0}^{n} \frac{1}{1+k} \sum_{j=0}^{k} (-1)^j \binom{k}{j} j^n, \quad \binom{k}{j} = \frac{k!}{j!(k-j)!},$$

$$B_n^+ = \sum_{k=0}^{n} \frac{1}{1+k} \sum_{j=0}^{k} (-1)^j \binom{k}{j} (j+1)^n,$$

$$B_m = 1 - \sum_{k=0}^{m-1} \binom{m}{k} \frac{B_k}{m-k+1}, \quad B_0 = 1.$$

The Bernoulli polynomials are defined by the generating function

$$G(x,t) = \frac{xe^{xt}}{e^x - 1} = \sum_{n=0}^{\infty} \frac{x^n}{n!} B_n(t).$$

The first few Bernoulli polynomials are defined as

$$B_0(t) = 1, \qquad B_1(t) = t - \frac{1}{2}, \qquad B_2(t) = t^2 - t + \frac{1}{6}, \qquad B_3(t) = t^3 - \frac{3}{2}t^2 + \frac{1}{2}t,$$

$$B_4(t) = t^4 - 2t^3 + t^2 - \frac{1}{30}, \qquad B_5(t) = t^5 - \frac{5}{2}t^4 + \frac{5}{3}t^3 - \frac{1}{6}t.$$

The initial group of GPs are listed as follows:

$$G_0(\xi) = 0, \quad G_1(\xi) = 1, \quad G_2(\xi) = 2\xi - 1, \quad G_3(\xi) = 3\xi^2 - 3\xi, \quad G_4(\xi) = 4\xi^3 - 6\xi^2 + 1, \quad G_5(\xi) = 5\xi^4 - 10\xi^3 + 5\xi.$$

Moreover,

$$\int_0^1 G_p(t)G_q(t)dt = \frac{2(-1)^p p!q!}{(p+q)!} G_{p+q}, \qquad p,q \geq 1,$$

$$\frac{dG_p(t)}{dt} = pG_{p-1}, \quad p \geq 1,$$

$$G_p(1) + G_p(0) = 0, \qquad p > 1,$$

$$G_p(t) = \int_0^t pG_{p-1}(t)dt + G_p, \quad p \geq 1.$$

Liu and Wang [30] studied certain identities of Bernoulli, Euler, and Genocchi polynomials using power sums and alternative power sums. For more details on the relations between Genocchi polynomials and Bernoulli polynomials, please see [30].

6.2. Function Approximation

The unknown function $\varphi(t)$ of Equation (5) can be expanded in terms of GPs as follows,

$$\varphi(t) \simeq \varphi_N(t) = \sum_{n=1}^{N} \varepsilon_n G_n(t), \tag{27}$$

where ε_n are unknown coefficients and $G_n(t)$ is GPs, which are defined by (26).

Substituting from (27) into (5) and using the collocation points

$$t_\ell = \frac{2\ell - 1}{2N}, \quad \ell = 1, 2, \ldots, N, \tag{28}$$

we obtain the next nonlinear system of algebraic equations

$$\int_0^{t_\ell} G(\alpha, t_\ell, s)\gamma\left(s, \sum_{n=1}^{N} \varepsilon_n G_n(s)\right) ds + \int_0^a k(t_\ell, z) \sum_{n=1}^{N} \varepsilon_n G_n(z)dz - \mu \sum_{n=1}^{N} \varepsilon_n G_n(t_\ell) = f(t_\ell). \tag{29}$$

By evaluating the unknown coefficients ε_n and applying the Newton iteration approach [31,32], we may resolve the nonlinear system (29).

Similarly, it is easy to obtain the approximate solution of Equations (6) and (7) in the same manner.

7. Numerical Examples

Two numerical examples with various values of α are provided in this section as an application of the findings above. All of the numerical computations were completed using the Maple 18 program.

Example 1. *Consider the NFrIE of the second kind:*

$$\frac{1}{\Gamma(\alpha)}\int_0^t (t-s)^{\alpha-1}s^5\varphi^2(s)ds+\int_0^1 t^2z^2\varphi(z)dz-\varphi(t)=f(t),\quad T\varphi(0)-\varphi(0)=0, \tag{30}$$

where the known function $f(t)$ is described by putting $\varphi(t)=t^4$ as an exact solution.

After using the value of the unknown function as an exact solution, we have f(t) in the form

$$\frac{\Gamma(10)}{\Gamma(10+\alpha)}t^{9+\alpha}-\frac{4}{5}t^2=f(t).$$

It is clear that the function $f(t)$ is bounded and continuous and $f(0)=0$.

In Example 1, we consider

$$\frac{d^\alpha}{dt^\alpha}\left\{\int_0^1 t^2z^2\varphi(z)dz-\varphi(t)\right\}=g(t)-\left(t^5\varphi^2(t)\right),$$

which is a special case from the general formula

$$\frac{d^\alpha}{dt^\alpha}(T\varphi(t)-\varphi(t))=g(t)-M(t)\gamma(\varphi(t)),\quad (T\varphi(0)-\varphi(0)=0),$$

where $T\varphi(t)-$ is an integral operator.

Now, applying GPM to Equation (30) and using the collocation point (28) for $N=5$, the approximate solution of Equation (30) can be collected in the next forms by varying the value of α:

$$\varphi(t)\simeq\varphi_5(t)=1.50\times10^{-8}-2.47\times10^{-7}t+0.1226\times10^{-5}t^2-0.2280\times10^{-7}t^3+1.000001458t^4,\alpha=0.00001,$$

$$\varphi(t)\simeq\varphi_5(t)=3\times10^{-10}-4\times10^{-9}t+1.4\times10^{-8}t^2-1.7\times10^{-8}t^3+1.000000007t^4,\quad \alpha=\frac{1}{5},$$

$$\varphi(t)\simeq\varphi_5(t)=3\times10^{-10}-4\times10^{-9}t+1.8\times10^{-8}t^2-2.6\times10^{-8}t^3+1.000000012t^4,\alpha=\frac{1}{4},$$

$$\varphi(t)\simeq\varphi_5(t)=2\times10^{-10}-3\times10^{-9}t+8\times10^{-9}t^2-6\times10^{-9}t^3+1.000000002t^4,\alpha=\frac{1}{3},$$

$$\varphi(t)\simeq\varphi_5(t)=1.0\times10^{-9}-7\times10^{-9}t+2.5\times10^{-8}t^2-3.8\times10^{-8}t^3+1.000000020t^4,\alpha=\frac{1}{2},$$

$$\varphi(t)\simeq\varphi_5(t)=1\times10^{-10}-3\times10^{-9}t^2+1.4\times10^{-8}t^3+0.9999999870t^4,\alpha=0.95.$$

Also, absolute errors are shown in Table 1 and Figures 1–8. A comparison between the exact solution and approximate solution of Example 1, $\alpha=1$ is shown in Figure 9.

Example 2. *Consider the integro-differential equation of the first order:*

$$\frac{d\varphi}{dt}-\varphi(t)-\frac{1}{\Gamma(\alpha)}\int_0^t (t-s)^{\alpha-1}s^5\varphi^3(s)ds=f(t),\qquad D\varphi(0)-\varphi(0)=0, \tag{31}$$

where the known function $f(t)$ is described by putting $\varphi(t)=t^2$ as an exact solution.

Table 1. Absolute errors (E) of Example 1.

t	E, α = 0.00001	E, $\alpha = \frac{1}{5}$	E, $\alpha = \frac{1}{4}$	E, $\alpha = \frac{1}{3}$	E, $\alpha = \frac{1}{2}$	E, α = 0.95
0	1.50×10^{-8}	3×10^{-10}	3×10^{-10}	2×10^{-10}	1×10^{-9}	1×10^{-10}
0.1	4.258×10^{-10}	2.37×10^{-11}	5.52×10^{-11}	2.58×10^{-11}	5.14×10^{-10}	8.27×10^{-11}
0.2	1.2672×10^{-9}	6.48×10^{-11}	3.12×10^{-11}	1.248×10^{-10}	3.28×10^{-10}	7.12×10^{-11}
0.3	1.4898×10^{-9}	4.23×10^{-11}	1.152×10^{-10}	1.258×10^{-10}	2.86×10^{-10}	1.027×10^{-10}
0.4	3.7648×10^{-9}	3.12×10^{-11}	2.232×10^{-10}	5.28×10^{-11}	2.8×10^{-10}	1.832×10^{-10}
0.5	4.1250×10^{-9}	1.125×10^{-10}	3.0×10^{-10}	7.50×10^{-11}	2.5×10^{-10}	2.875×10^{-10}
0.6	4.6368×10^{-9}	1.752×10^{-10}	3.192×10^{-10}	2.432×10^{-10}	1.84×10^{-10}	3.592×10^{-10}
0.7	1.08658×10^{-8}	2.097×10^{-10}	2.832×10^{-10}	4.422×10^{-10}	1.18×10^{-10}	3.107×10^{-10}
0.8	3.18768×10^{-8}	2.232×10^{-10}	2.232×10^{-10}	6.672×10^{-10}	1.36×10^{-10}	2.32×10^{-11}
0.9	8.02338×10^{-8}	2.397×10^{-10}	1.992×10^{-10}	9.182×10^{-10}	3.7×10^{-10}	6.533×10^{-10}
1	1.720×10^{-7}	3×10^{-10}	3×10^{-10}	1.2×10^{-9}	1×10^{-9}	1.9×10^{-9}

In Example 2, we consider

$$\frac{d^\alpha}{dt^\alpha}\left\{\frac{d\varphi(t)}{dt} - \varphi(t)\right\} = g(t) - \left(t^5\varphi^3(t)\right),$$

$$\frac{d^\alpha}{dt^\alpha}\{D\varphi(t) - \varphi(t)\} = g(t) - M(t)\gamma(\varphi(t)), \quad (D\varphi(0) - \varphi(0) = 0),$$

where $D\varphi(t)-$ is a differentiable operator.

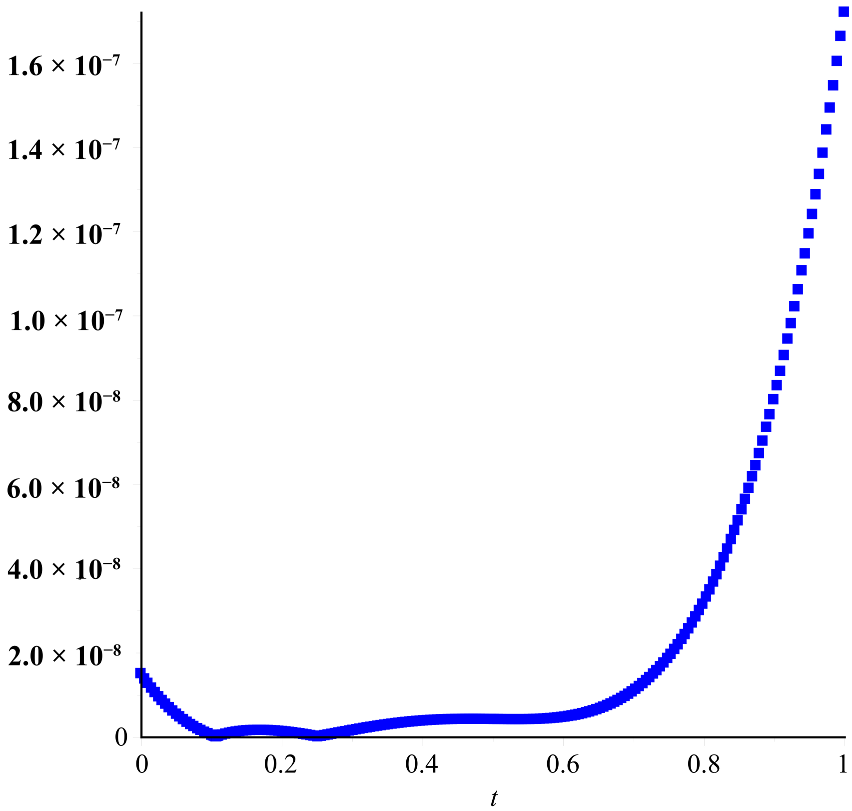

Figure 1. Absolute error of Example 1, $\alpha = 0.00001$.

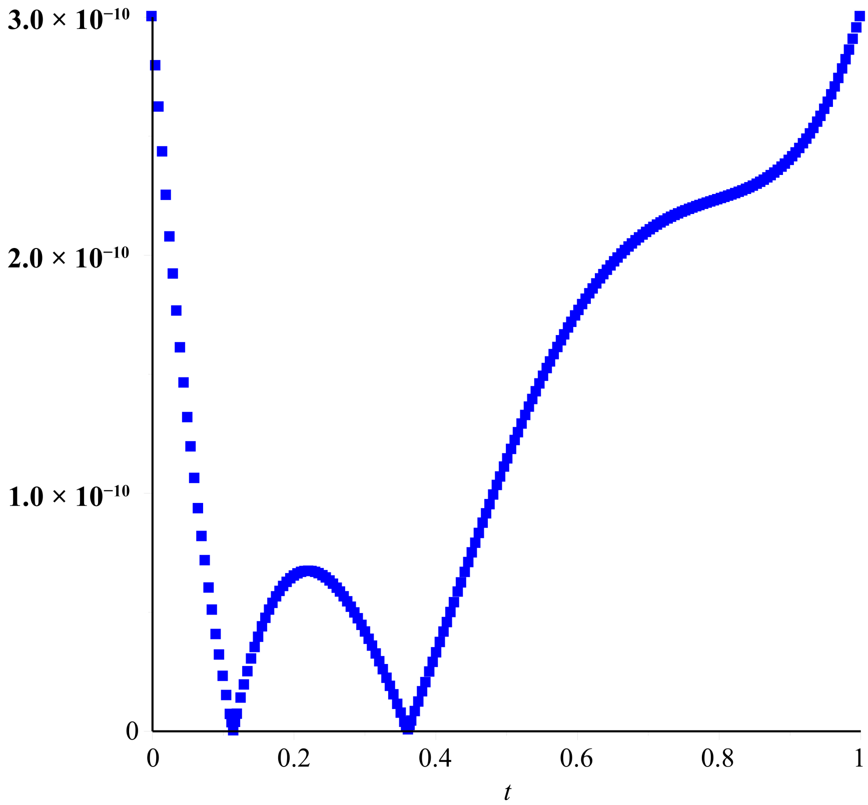

Figure 2. Absolute error of Example 1, $\alpha = \frac{1}{5}$.

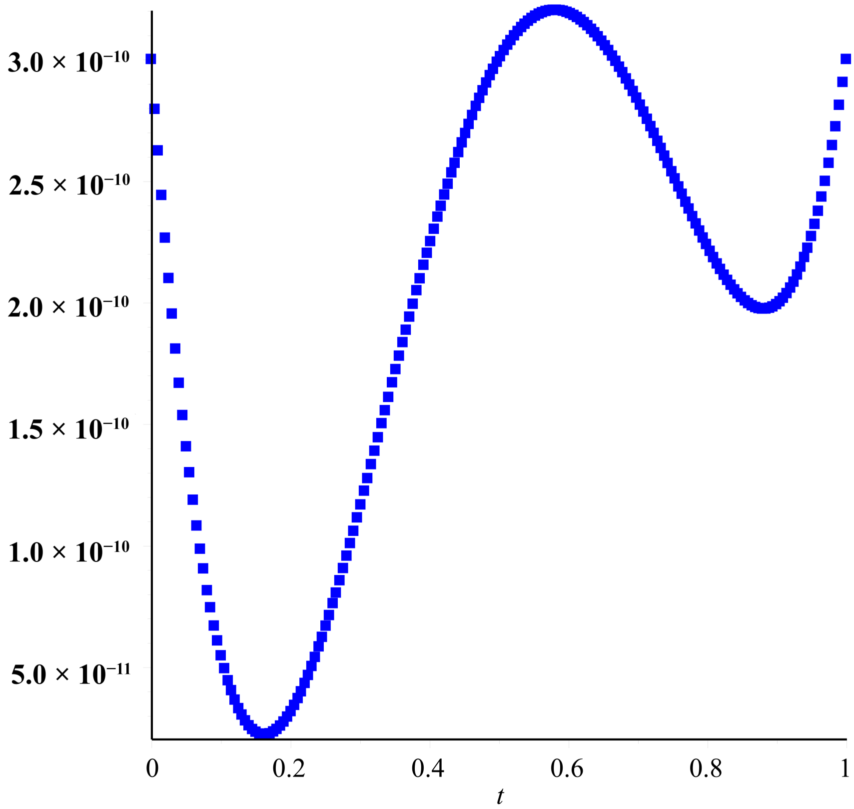

Figure 3. Absolute error of Example 1, $\alpha = \frac{1}{4}$.

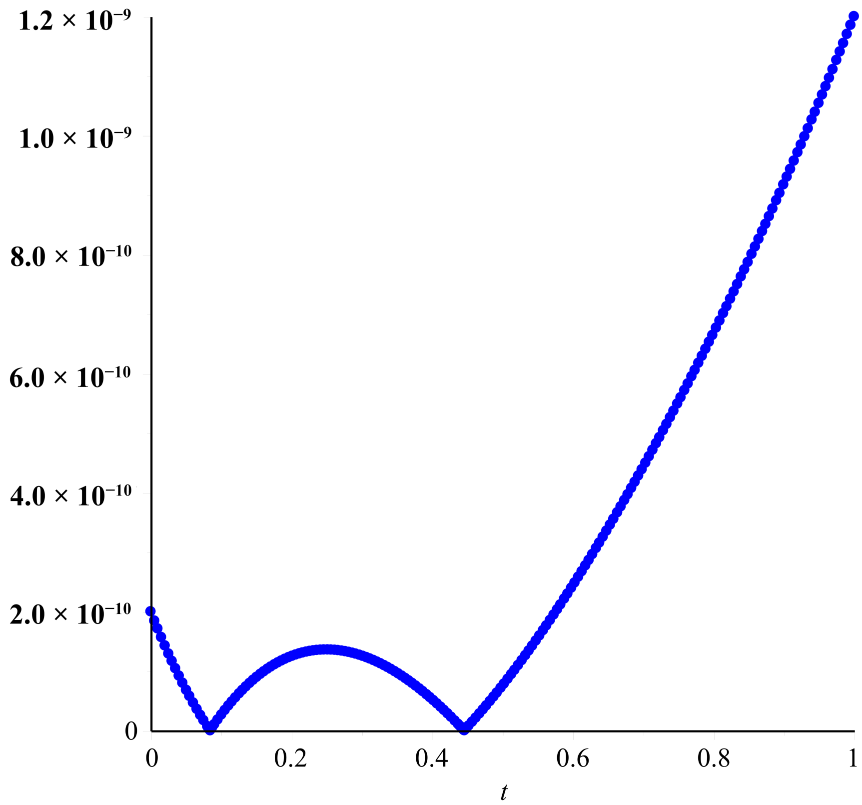

Figure 4. Absolute error of Example 1, $\alpha = \frac{1}{3}$.

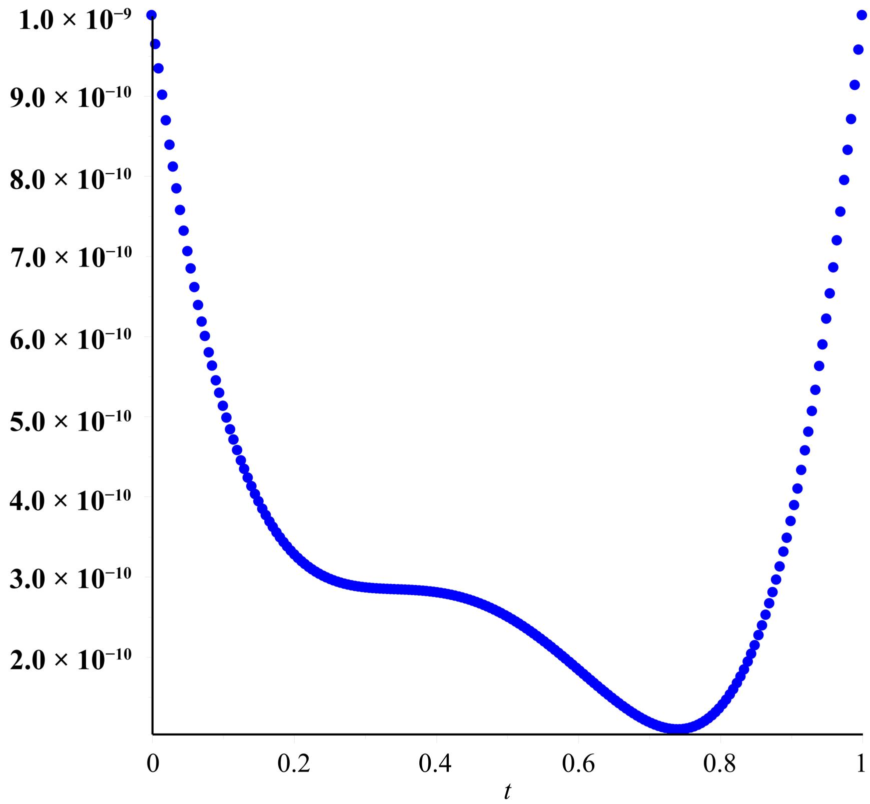

Figure 5. Absolute error of Example 1, $\alpha = \frac{1}{2}$.

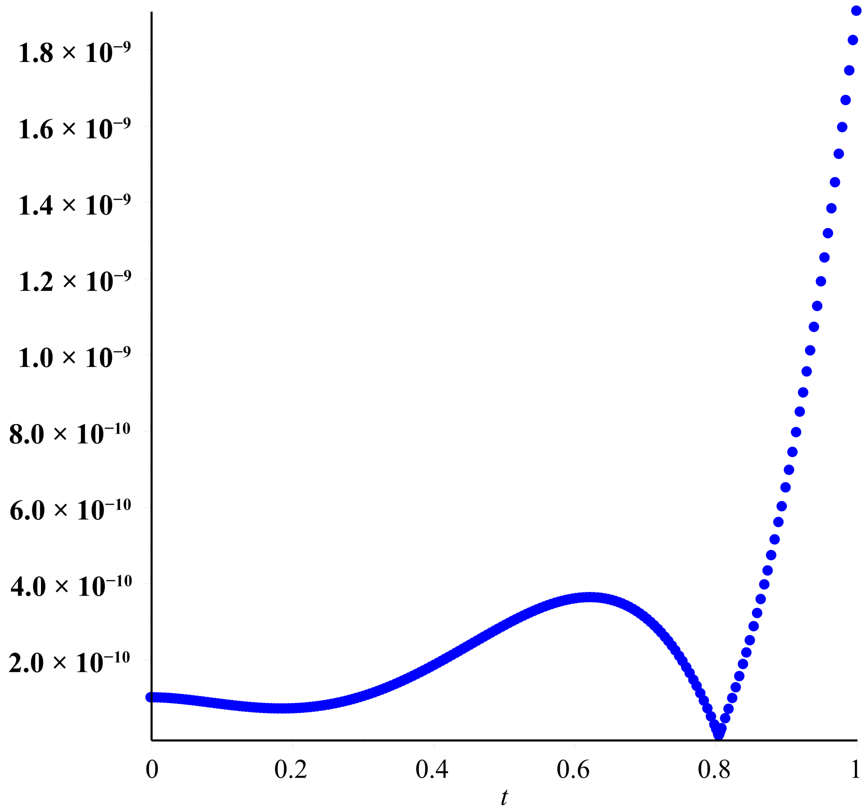

Figure 6. Absolute error of Example 1, $\alpha = 0.95$.

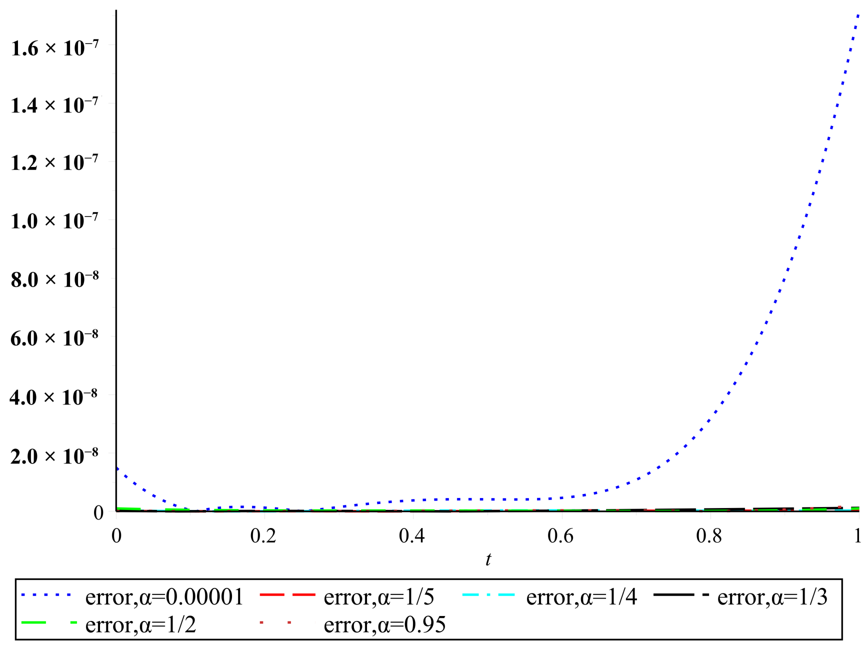

Figure 7. Comparison between the absolute errors of Example 1.

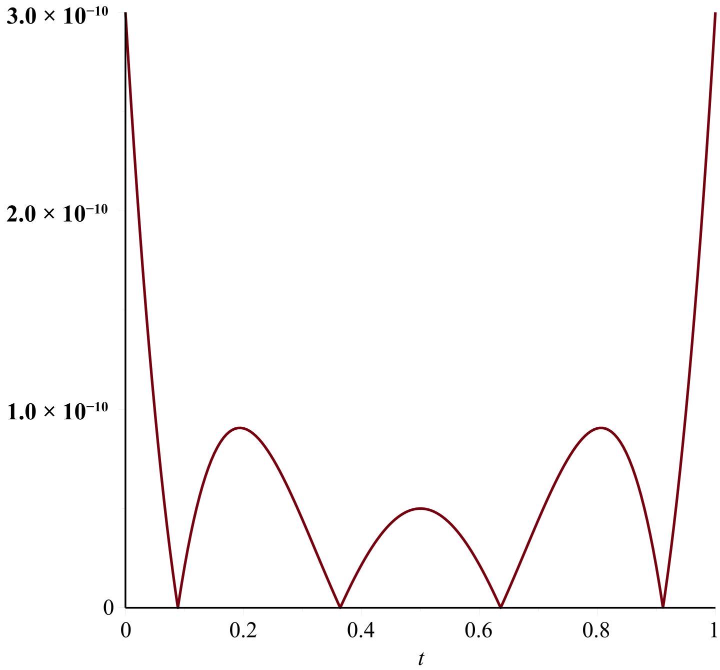

Figure 8. Absolute error of Example 1, $\alpha = 1$.

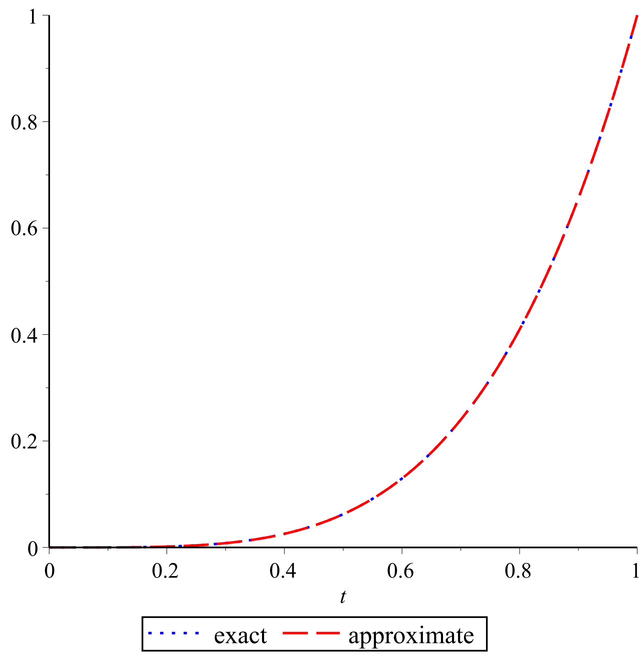

Figure 9. Comparison between exact solution and approximate solution of Example 1, $\alpha = 1$.

Similar to in Example 1, applying GPM to Equation (31) and using the collocation point (28) for $N = 5$, the approximate solution of Equation (31) can be collected in several different formats by varying the value of α:

$$\varphi(t) \simeq \varphi_5(t) = 5.78926571 \times 10^{-11} + 1.000000000 \times t^2 - 6.58944122 \times 10^{-10} t^3 + 8.452573750 \times 10^{-10} t^4, \alpha = 0.00001,$$

$$\varphi(t) \simeq \varphi_5(t) = 1.347313885 \times 10^{-10} + 1 \times 10^{-9} t + 1.000000000 \times t^2 - 9.198107540 \times 10^{-10} t^3$$
$$+7.293681540 \times 10^{-10} t^4, \quad \alpha = \frac{1}{5},$$

$$\varphi(t) \simeq \varphi_5(t) = 2.386554161 \times 10^{-11} + 0.9999999998 \times t^2 + 2.143753015 \times 10^{-10} t^3 - 5.945656755 \times 10^{-11} t^4, \alpha = \frac{1}{4},$$

$$\varphi(t) \simeq \varphi_5(t) = -1.486305278 \times 10^{-11} + 1.000000000 \times t^2 + 1.708136551 \times 10^{-10} t^3 - 1.151329331 \times 10^{-10} t^4, \alpha = \frac{1}{3},$$

$$\varphi(t) \simeq \varphi_5(t) = -5.026134044 \times 10^{-11} - 2 \times 10^{-10} t + 0.9999999999 \times t^2 + 2.168003276 \times 10^{-10} t^3 - 2.089228447 \times 10^{-10} t^4, \alpha = \frac{1}{2},$$

$$\varphi(t) \simeq \varphi_5(t) = -5.747226027 \times 10^{-10} - 4 \times 10^{-10} t + 0.9999999991 t^2 + 1.193531824 \times 10^{-9} t^3 - 7.462111175 \times 10^{-10} t^4, \alpha = 0.95.$$

Absolute errors are shown in Table 2 and Figures 10–16.

Table 2. Absolute errors of Example 2.

t	E, α = 0.00001	E, $\alpha = \frac{1}{5}$	E, $\alpha = \frac{1}{4}$	E, $\alpha = \frac{1}{3}$	E, $\alpha = \frac{1}{2}$	E, α = 0.95
0	5.78×10^{-11}	1.34×10^{-10}	2.38×10^{-11}	1.48×10^{-11}	5.02×10^{-11}	5.74×10^{-10}
0.1	5.73×10^{-11}	2.33×10^{-10}	2.20×10^{-11}	1.47×10^{-11}	7.10×10^{-11}	6.22×10^{-10}
0.2	5.39×10^{-11}	3.28×10^{-10}	1.74×10^{-11}	1.36×10^{-11}	9.28×10^{-11}	6.82×10^{-10}
0.3	4.69×10^{-11}	4.15×10^{-10}	1.11×10^{-11}	1.11×10^{-11}	1.15×10^{-10}	7.49×10^{-10}
0.4	3.73×10^{-11}	4.94×10^{-10}	4.06×10^{-12}	6.87×10^{-12}	1.37×10^{-10}	8.21×10^{-10}
0.5	2.83×10^{-11}	5.65×10^{-10}	3.05×10^{-12}	7.07×10^{-13}	1.61×10^{-10}	8.97×10^{-10}
0.6	2.51×10^{-11}	6.30×10^{-10}	9.53×10^{-12}	7.11×10^{-12}	1.86×10^{-10}	9.77×10^{-10}
0.7	3.48×10^{-11}	6.94×10^{-10}	1.48×10^{-11}	1.60×10^{-11}	2.15×10^{-10}	1.06×10^{-9}
0.8	6.67×10^{-11}	7.62×10^{-10}	1.87×10^{-11}	2.54×10^{-11}	2.48×10^{-10}	1.16×10^{-9}
0.9	1.32×10^{-10}	8.42×10^{-10}	2.08×10^{-11}	3.41×10^{-11}	2.90×10^{-10}	1.28×10^{-9}
1	2.44×10^{-10}	9.44×10^{-10}	2.12×10^{-11}	4.08×10^{-11}	3.42×10^{-10}	1.42×10^{-9}

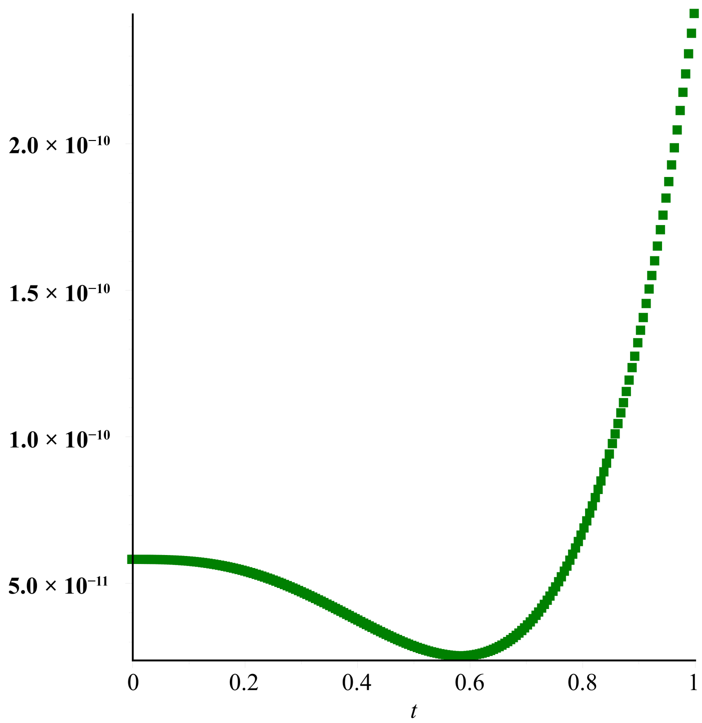

Figure 10. Absolute error of Example 2, $\alpha = 0.00001$.

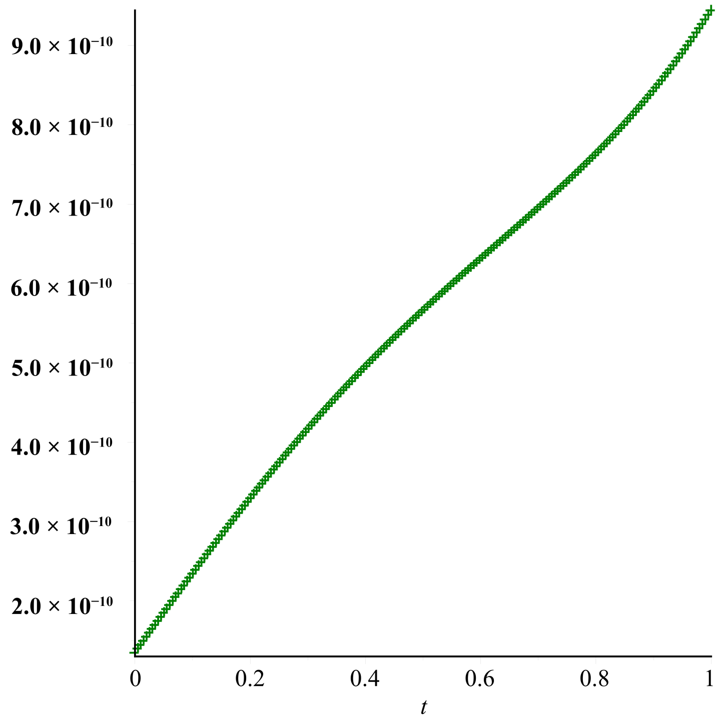

Figure 11. Absolute error of Example 2, $\alpha = \frac{1}{5}$.

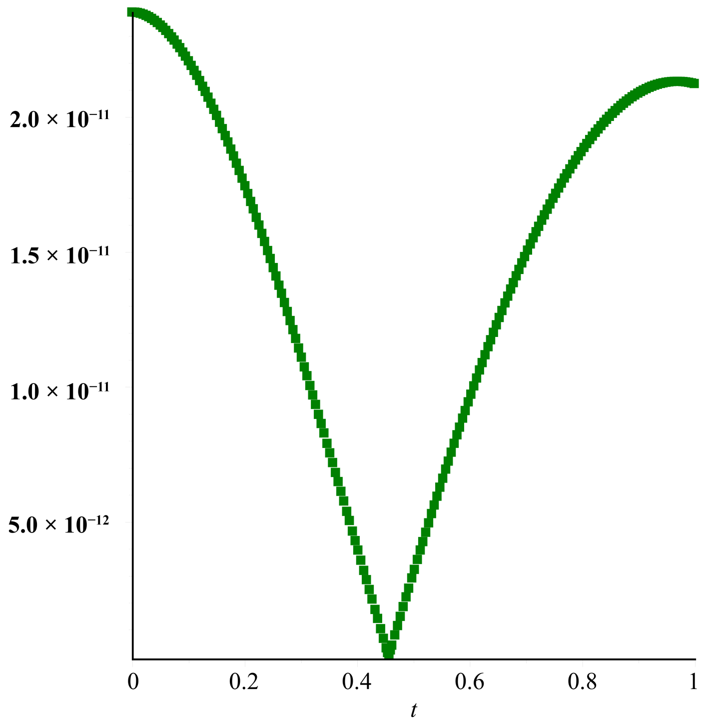

Figure 12. Absolute error of Example 2, $\alpha = \frac{1}{4}$.

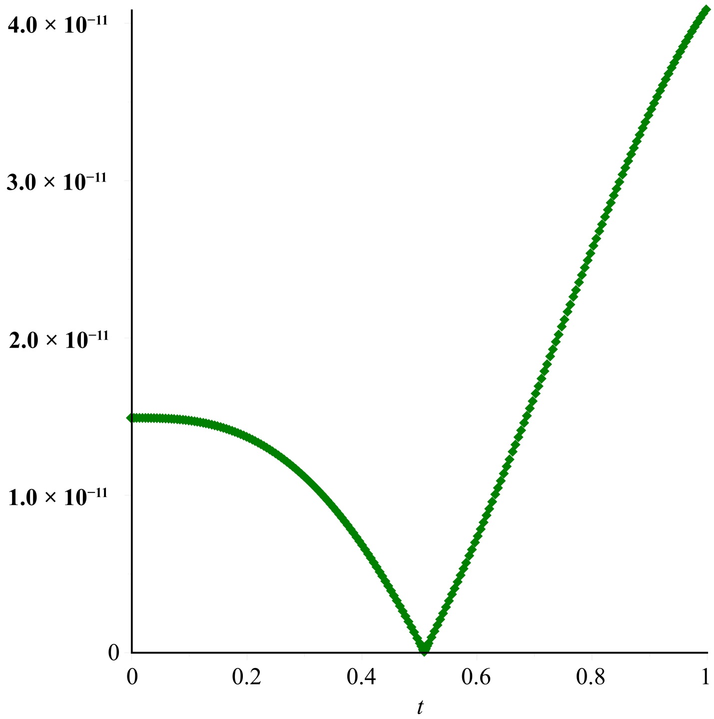

Figure 13. Absolute error of Example 2, $\alpha = \frac{1}{3}$.

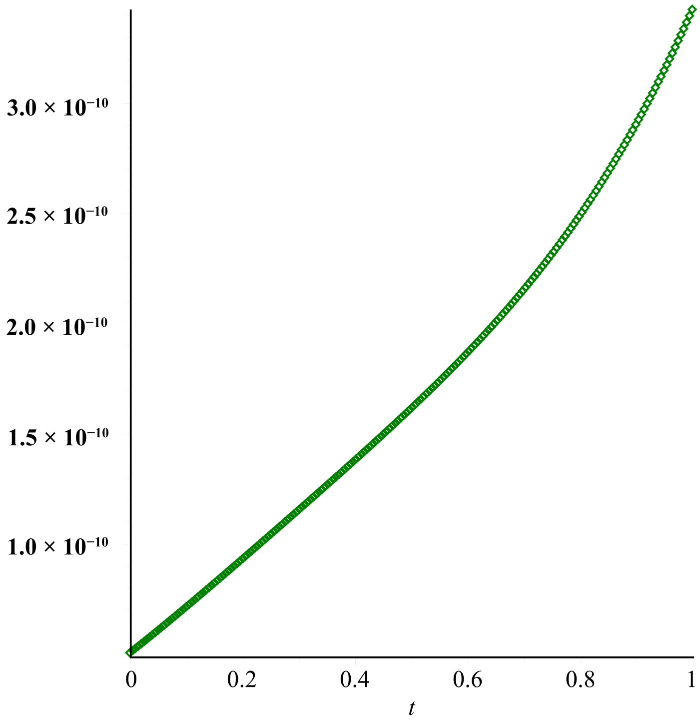

Figure 14. Absolute error of Example 2, $\alpha = \frac{1}{2}$.

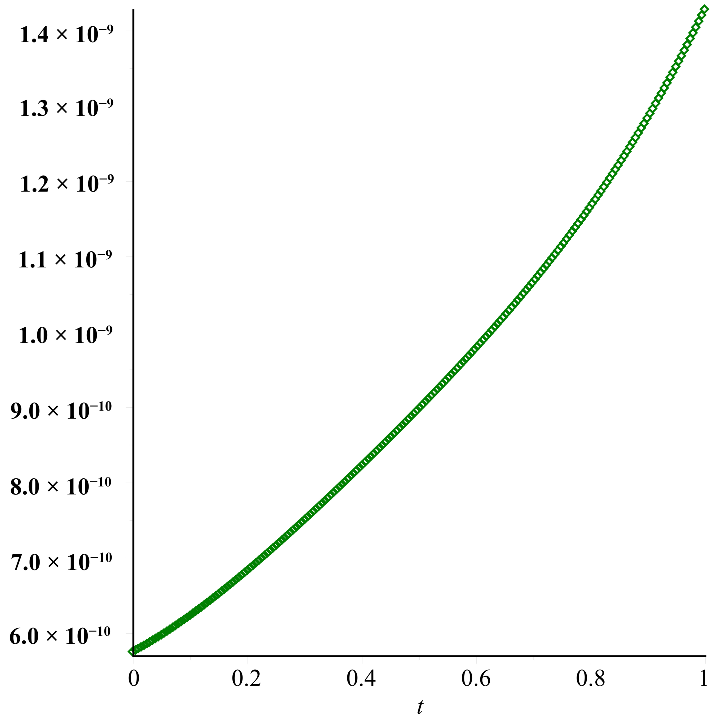

Figure 15. Absolute error of Example 2, $\alpha = 0.95$.

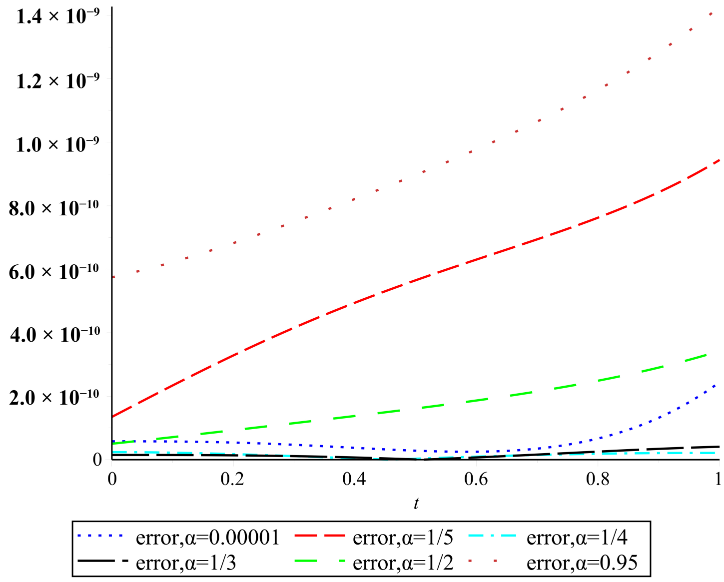

Figure 16. Comparison between the absolute errors of Example 2.

8. Discussion of the Results

Two numerical examples are presented: Example 1, applied to the first application Equation (5), and Example 2, applied to the integro-differential equation of the first order (7) when the operator T is differentiable. We note that

1. In Example 1, the largest error value at $\alpha = 0.00001, t = 1$ is 1.720×10^{-7} but at all different values of α at $t = 1$ the error values equal constant $\times 10^{-9}$ and constant at $\times 10^{-10}$; this is clear in Table 3.

Table 3. The largest error value of example 1.

t	E, α = 0.00001	E, $\alpha = \frac{1}{5}$	E, $\alpha = \frac{1}{4}$	E, $\alpha = \frac{1}{3}$	E, $\alpha = \frac{1}{2}$	E, α = 0.95
1	1.720×10^{-7}	3×10^{-10}	3×10^{-10}	1.2×10^{-9}	1×10^{-9}	1.9×10^{-9}

The lowest value for error at $\alpha = 0.00001, t = 0.1$ is 4.258×10^{-10} but at all different values of α at $t = 0.1$ the error values equal constant $\times 10^{-11}$, except at $\alpha = \frac{1}{2}$ where the error equals 5.14×10^{-10}; this is clear in Table 4.

Table 4. The lowest error value of example 1.

t	E, α = 0.00001	E, $\alpha = \frac{1}{5}$	E, $\alpha = \frac{1}{4}$	E, $\alpha = \frac{1}{3}$	E, $\alpha = \frac{1}{2}$	E, α = 0.95
0.1	4.258×10^{-10}	2.37×10^{-11}	5.52×10^{-11}	2.58×10^{-11}	5.14×10^{-10}	8.27×10^{-11}

In Figure 1, at $\alpha = 0.00001$ the absolute errors equal constant $\times 10^{-7}$ and constant $\times 10^{-8}$, while in Figure 2 at $\alpha = 0.2$ the absolute errors equal constant $\times 10^{-10}$, and also in Figure 3 at $\alpha = 0.25$ the absolute errors equal constant $\times 10^{-10}$ and constant $\times 10^{-11}$, while in Figures 4–6 at $\alpha = \frac{1}{3}, \frac{1}{2}, 0.95$ the absolute errors equal constant $\times 10^{-9}$ and constant $\times 10^{-10}$. A comparison between the absolute errors for different values of α of Example 1 are presented in Figure 7. Figure 8 represents the absolute errors, $\alpha = 1$, and the comparison between the exact solution and approximate solution is represented in Figure 9 at $\alpha = 1$.

2. In example 2, the lowest value for error at $\alpha = \frac{1}{3}, t = 0.5$ is 7.07×10^{-13}.

Table 5. The lowest error value of Example 2.

t	E, α = 0.00001	E, $\alpha = \frac{1}{5}$	E, $\alpha = \frac{1}{4}$	E, $\alpha = \frac{1}{3}$	E, $\alpha = \frac{1}{2}$	E, α = 0.95
0.5	2.83×10^{-11}	5.65×10^{-10}	3.05×10^{-12}	7.07×10^{-13}	1.61×10^{-10}	8.97×10^{-10}

Table 6. The largest error value of Example 2.

t	E, α = 0.00001	E, $\alpha = \frac{1}{5}$	E, $\alpha = \frac{1}{4}$	E, $\alpha = \frac{1}{3}$	E, $\alpha = \frac{1}{2}$	E, α = 0.95
1	2.44×10^{-10}	9.44×10^{-10}	2.12×10^{-11}	4.08×10^{-11}	3.42×10^{-10}	1.42×10^{-9}

In Figure 10, at $\alpha = 0.00001$ the absolute errors equal constant $\times 10^{-10}$ and constant $\times 10^{-11}$, while in Figure 11 at $\alpha = 0.2$ the absolute errors equal constant $\times 10^{-10}$, while in Figure 12 at $\alpha = 0.25$ the absolute errors equal constant $\times 10^{-11}$ and constant $\times 10^{-12}$. In Figure 13 at $\alpha = \frac{1}{3}$ the absolute errors equal constant $\times 10^{-11}$, in Figure 14 at $\alpha = \frac{1}{2}$ the absolute errors equal constant $\times 10^{-10}$, while in Figure 15 at $\alpha = 0.95$ the absolute errors equal constant $\times 10^{-9}$ and constant $\times 10^{-10}$. A comparison between the absolute errors of different values of α in Example 2 are presented in Figure 16. In Example 2, we have demonstrated less error value in Table 5, also, we have demonstrated the largest error value in Table 6.

9. Conclusions

In the present paper, the Genocchi polynomial method was applied to solve NFrIEs of the second kind. The Genocchi polynomial method converted the problem to a system of algebraic equations. Finally, two numerical examples were discussed to demonstrate the applicability and validity of the method. We have shown the existence of a unique solution to the second sort of NFrIE in Hilbert space. Furthermore, we have explained and discussed proof of the stability of the error.

Future Works

We will study and extend the work using some different numerical methods and also some semi-analytical methods.

Author Contributions: Conceptualization, A.M.S.M.; Methodology, A.M.S.M., M.A.A. and D.S.M.; Software, R.T.M., A.M.S.M., M.A.A. and D.S.M.; Formal analysis, D.S.M.; Resources, R.T.M., A.M.S.M. and D.S.M.; Data curation, A.M.S.M.; Writing—original draft, R.T.M., A.M.S.M., M.A.A. and D.S.M.; Writing—review & editing, R.T.M., A.M.S.M., M.A.A. and D.S.M.; Supervision, A.M.S.M. and M.A.A.; Funding acquisition, R.T.M. All authors have read and agreed to the published version of the manuscript.

Funding: This research received no external funding.

Institutional Review Board Statement: Not applicable.

Informed Consent Statement: Not applicable.

Data Availability Statement: No new data were created or analyzed in this study. Data sharing is not applicable to this article.

Acknowledgments: The authors express their gratitude to the editor and the anonymous referees for their critical reading of the paper and their insightful remarks, which significantly enhanced it.

Conflicts of Interest: The authors declare no conflict of interest.

References

1. Hamdan, S.; Qatanani, N.; Daraghmeh, A. Numerical techniques for solving linear Volterra fractional integral equation. *J. Appl. Math.* **2019**, *2019*, 5678103. [CrossRef]
2. Pu, T.; Fasondini, M. The numerical solution of fractional integral equations via orthogonal polynomials in fractional powers. *Adv Comput Math.* **2023**, *49*, 1–40. [CrossRef]
3. Bekkouche, M.M.; Mansouri, I.; Azeb Ahmed, A.A. Numerical solution of fractional boundary value problem with caputo-fabrizio and its fractional integral. *J. Appl. Math. Comput.* **2022**, *68*, 4305–4316. [CrossRef] [PubMed]
4. Mahdy, A.M.S.; Nagdy, A.S.; Mohamed, D.S. Solution of fractional integro-differential equations using least squares and shifted legendre methods. *J. Appl. Math. Comput. Mech.* **2024**, *23*, 59–70. [CrossRef]
5. Alsulaiman, R.E.; Abdou, M.A.; Youssef, E.M.; Taha, M. Solvability of a nonlinear integro-differential equation with fractional order using the Bernoulli matrix approach. *AIMS Math.* **2023**, *8*, 7515–7534. [CrossRef]
6. Alharbi, F.M.; Zidan, A.M.; Naeem, M.; Shah, R.; Nonlaopon, K. Numerical investigation of fractional-order differential equations via φ-Haar-Wavelet method. *J. Funct. Spaces* **2021**, *2021*, 3084110. [CrossRef]
7. Mohamed, D.S.; Abdou, M.A.; Mahdy, A.M.S. Dynamical investigation and numerical modeling of a fractional mixed nonlinear partial integro-differential problem in time and space. *J. Appl. Anal. Comput.* **2024**, *14*, 1–21.
8. Zabidi, N.A.; Majid, Z.A.; Kilicman, A.; Ibrahim, Z.B. Numerical solution of fractional differential equations with Caputo derivative by using numerical fractional predict-correct technique. *Adv. Contin. Discret. Model.* **2022**, *2022*, 1–23. [CrossRef]
9. Yi, X.; Liu, C.; Cheong, H.T.; Teo, K.L.; Wang, S. A third-order numerical method for solving fractional ordinary differential equations. *AIMS Math.* **2024**, *9*, 21125–21143. [CrossRef]
10. Jassim, H.K.; Hussein, M.A. A New approach for solving nonlinear fractional ordinary differential equations. *Mathematics* **2023**, *11*, 1565. [CrossRef]
11. Mohamed, M.Z.; Yousif, M.; Hamza, A.E. Solving nonlinear fractional partial differential equations using the elzaki transform method and the homotopy perturbation method. In *Abstract and Applied Analysis*; John Wiley & Sons, Inc.: Hoboken, NJ, USA, 2022; pp. 1–9.
12. Rashid, S.; Ahmad, A.G.; Jarad, F.; Alsaadi, A. Nonlinear fractional differential equations and their existence via fixed point theory concerning to Hilfer generalized proportional fractional derivative. *AIMS Math.* **2022**, *8*, 382–403. [CrossRef]
13. Lydia, S.K.; Jancirani, M.M.; Anitha, A.A. Numerical solution of nonlinear fractional differential equations using kharrat-toma iterative method. *Nat. Volatiles Essent. Oils* **2021**, *8*, 9878–9890.
14. Yu, C. A Study on a nonlinear fractional differential equation. *Int. J. Nov. Res. Comput. Sci. Softw. Eng.* **2023**, *10*, 28–33.
15. Dehestani, H.; Ordokhani, Y.; Razzaghi, M. The novel operational matrices based on 2D-Genocchi polynomials: Solving a general class of variable-order fractional partial integro-differential equations. *Comput. Appl. Math.* **2020**, *39*, 259. [CrossRef]
16. Khajehnasiri, A.; Ebadian, A. Genocchi operational matrix method and their applications for solving fractional weakly singular two-dimensional partial Volterra integral equation. *UPB Sci. Bull. Ser. A* **2023**, *85*, 155–170.
17. Loh, J.R.; Phang, C.; Isah, A. Numerical solution for arbitrary domain of fractional integro-differential equation via the general shifted Genocchi polynomials. *J. Funct. Spaces* **2020**, *2023*, 5921425. [CrossRef]

18. Ebrahimzadeh, A.; Hashemizadeh, E. Optimal control of nonlinear Volterra integral equations with weakly singular kernels based on Genocchi polynomials and collocation method. *J. Nonlinear Math. Phys.* **2023**, *30*, 1758–1773. [CrossRef]
19. Hashemizadeh, E.; Ebadi, M.A.; Noeiaghdam, S. Matrix method by Genocchi polynomials for solving nonlinear Volterra integral equations with weakly singular kernels. *Symmetry* **2020**, *12*, 2105. [CrossRef]
20. Heydari, M.H.; Zhagharian, S. Genocchi polynomials for variable order time fractional Fornberg Whitham type equations. *Partial. Differ. Equ. Appl. Math.* **2023**, *8*, 100554. [CrossRef]
21. Loh, J.R.; Phang, C.; Isah, A. New operational matrix via Genocchi polynomials for solving Fredholm-Volterra fractional integro-differential equations. *Adv. Math. Phys.* **2017**, *2017*, 3821870. [CrossRef]
22. Seghiri, N.; Nadir, M.; Khirani, A. Operational matrices of Genocchi polynomials for solving high-order linear Fredholm integro-differential equations. *Math. Model. Eng. Probl.* **2024**, *11*, 2473–2482. [CrossRef]
23. Mustapha, D. Numerical solution of integro-differential equations of the second kind by using Galerkin's method with Genocchi polynomial. *J. Jilin Univ. (Eng. Technol. Ed.)* **2024**, *43*, 60–70.
24. Isah, A.; Phang, C. New operational matrix of derivative for solving non-linear fractional differential equations via Genocchi polynomials. *J. King Saud Univ. Sci.* **2019**, *31*, 1–7. [CrossRef]
25. Granos, A.; Dugundji, J. *Fixed Point Theorem*; Springer: New York, NY, USA, 2003.
26. Hilfar, R. *Application of Fractional Calculus in Physics*; World Scientific: Singapore, 2000.
27. Kilbas, A.A.; Srivastava, H.M.; Trullo, J.J. *Theory and Applications of Fractional Differential Equations*; Elsevier Science B.V.: Amsterdam, The Netherlands, 2006; North-Holland Mathematics Studies.
28. Abdou, M.A.; Salama, F.A. Fredholm-Volterra integral equation of the first kind and spectral relationships. *Appl. Math. Comput.* **2004**, *153*, 141–153. [CrossRef]
29. Abdou, M.A. Fredholm-Volterra integral equation of the first kind and contact problem. *Appl. Math. Comput.* **2002**, *125*, 177–193. [CrossRef]
30. Liu, H.; Wang, W. Some identities on the Bernoulli, Euler and Genocchi polynomials via power sums and alternate power sums. *Discret. Math.* **2009**, *309*, 3346–3363. [CrossRef]
31. Smith, G.D. *Numerical Solution of Partial Differential Equations: Finite Difference Methods*, 3rd ed.; Oxford University Press: Oxford, UK, 1985.
32. Morton, K.W.; Mayers, D.F. *Numerical Solution of Partial Differential Equations*; Cambridge University Press: Cambridge, UK, 1994.